

Measurements of critical current diffraction patterns in annular Josephson junctions

Andreas Franz, Andreas Wallraff, and Alexey V. Ustinov

Physikalisches Institut III, Universität Erlangen-Nürnberg, D-91058 Erlangen, Germany

(November 21, 2018)

We report systematic measurements of the critical current versus magnetic field patterns of annular Josephson junctions in a wide magnetic field range. A modulation of the envelope of the pattern, which depends on the junction width, is observed. The data are compared with theory and good agreement is found.

74.50.+r, 05.45.Yv, 85.25.Cp

Large area Josephson junctions are intriguing objects for performing experiments on nonlinear electrodynamics. In particular, the propagation of solitons, also called Josephson vortices or fluxons, has attracted a lot of attention and has been studied in detail.¹ Recently large area Josephson junctions have been proposed to be used as efficient radiation and particle detectors.²⁻⁴ In such junctions, the spatial dependence of the phase difference between the superconducting electrodes is an important characteristic that determines the junction properties.

In an annular Josephson junction, magnetic flux quanta threading one superconducting loop but not the other, are trapped and stored in the junction due to the fluxoid quantization.⁵ This property of the system offers the unique possibility to study fluxon dynamics in the absence of collisions with boundaries.⁶ In the annular junctions proposed^{3,4} for radiation and particle detection, trapped vortices are useful to suppress the critical current of the junction in order to allow for a stable bias point in the subgap region of the junction current-voltage characteristic.

In this report, we present systematic measurements of the critical current of annular Josephson junctions in dependence on the externally applied in-plane magnetic field. The critical current I_c of a junction without trapped fluxons is at maximum when no magnetic fields are present. In the presence of a magnetic field this maximum superconducting current is reduced. Magnetic fields can be due to the bias current applied to the junction (self-fields), due to flux trapped in the junction itself or its leads (Josephson or Abrikosov vortices, respectively), or they can be applied externally. The modulation of the critical current with the external field is often called a critical current diffraction pattern. We investigate these patterns for annular junctions of various dimensions in a wide range of magnetic fields.

We present experimental data on five annular Josephson junctions with the same external radius $r_e = 50 \mu\text{m}$ but different inner radii r_i ranging from 30 to 47 μm , see second and third column of Tab. I. Hence the width $w = r_e - r_i$ of the junctions is ranging from 3 to 20 μm . The junction geometry is shown in Fig. 1. All junctions have been prepared on the same chip using Hypres

TABLE I. Geometrical parameters and fitted values of the measured annular Josephson junctions.

junction #	r_i [μm]	$\delta = r_i/r_e$	$\Delta H'/\Delta H$	$2r_e/w$	$\tilde{\delta}$	Δr [μm]
A	47	0.94	-	-	0.96	0.5
B	45	0.9	22.9	20.0	0.92	0.5
C	42	0.84	13.2	12.5	0.88	1.0
D	35	0.7	6.5	6.7	0.72	0.6
E	30	0.6	4.8	5.0	0.62	0.5

junction #	\tilde{H}_0 [Oe]	\tilde{H}_0/H_0	$\tilde{\Lambda}$ [nm]
A	0.319	0.65	208
B	0.346	0.703	193
C	0.321	0.646	210
D	0.405	0.821	165
E	0.376	0.765	177

technology⁷ with a nominal critical current density of $j_c = 100 \text{ A/cm}^2$. Accordingly, the Josephson length is approximately 30 μm at 4.2 K.

In Fig. 2 the critical current diffraction patterns of the two junctions B and D, being representative for the set of measured samples, are shown. Obviously, a strong dependence of the pattern on the junction width is observed. As expected, the critical current of the junction at zero field scales with the junction size as $I_c = j_c 2\pi(r_e^2 - r_i^2)$. Measuring the diffraction patterns in a wide range of magnetic field, two characteristic modulation scales of the critical current are observed. The pattern having a small magnetic field period ΔH has an envelope of the larger period $\Delta H'$ which depends strongly on the width of the junction (compare Figs. 2a and b).

The observed critical current diffraction patterns can be qualitatively understood in the following way. The modulation of the period ΔH is due to the penetration of magnetic flux in the direction perpendicular to the external magnetic field. This period is inversely proportional to the diameter of the junction: $\Delta H \propto 1/(2r_e)$. This is analogous to the standard case, where ΔH is proportional to the reciprocal junction length in the direction perpendicular to the magnetic field.⁸ The minima of the modulation of the period $\Delta H'$ occur, when the magnetic flux penetrates the junction strongly also along the *width* of the junction. Therefore, the period $\Delta H'$ of the second

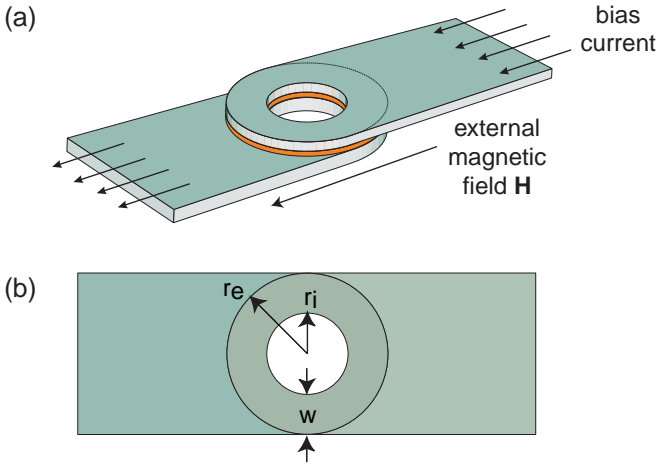


FIG. 1. Schematic of the annular Josephson junction biased in the Lyngby-geometry⁵ (a) and its dimensions (b).

modulation is proportional to $1/w$. By calculating the ratio

$$\frac{\Delta H'}{\Delta H} = \frac{2r_e}{w}, \quad (1)$$

for the different junctions, this simple prediction can be quantitatively compared with experiment. As can be seen from the fourth and fifth column of Tab. I, Eq. (1) is quite accurately fulfilled for our junctions.⁹

The described effect can be illustrated by plotting the supercurrent density j_s at different magnetic fields versus the junction coordinates. At the magnetic field $H = 3.25$ Oe $< \Delta H'$, approximately two and a half flux quanta penetrate into the junction cross section $2r_e$, as shown in the inset I of Fig. 2b. At the larger field $H = 12.2$ Oe $> \Delta H'$, more than one flux quantum penetrates the width cross section of the junction (see inset II of Fig. 2b). Thus, after each period $\Delta H'$, one additional flux quantum has penetrated the width of the junction. We note here, that the spatial distribution of the supercurrent density could also be measured in experiment.¹⁰

Several approaches to calculate the critical current diffraction patterns of annular Josephson junctions have been published earlier.^{11–13} Mainly, two different cases have been considered, the long annular Josephson junction with a circumference $2\pi\bar{r}$ larger than the Josephson length λ_J and the small annular Josephson junction where $2\pi\bar{r} < \lambda_J$,¹¹ where $\bar{r} = (r_i + r_e)/2$ is the mean radius of the junction.

The most complete theoretical description of the critical current diffraction pattern $I_c(H)$ of small annular junctions of arbitrary width and number of trapped fluxons n is presented by Nappi in Ref. 13. The dependence of the critical current I_c on the magnetic field H is given by the formula

$$I_c = I_0 \left| \frac{2}{1 - \delta^2} \int_{\delta}^1 x J_n \left(x \frac{H}{H_0} \right) dx \right|, \quad (2)$$

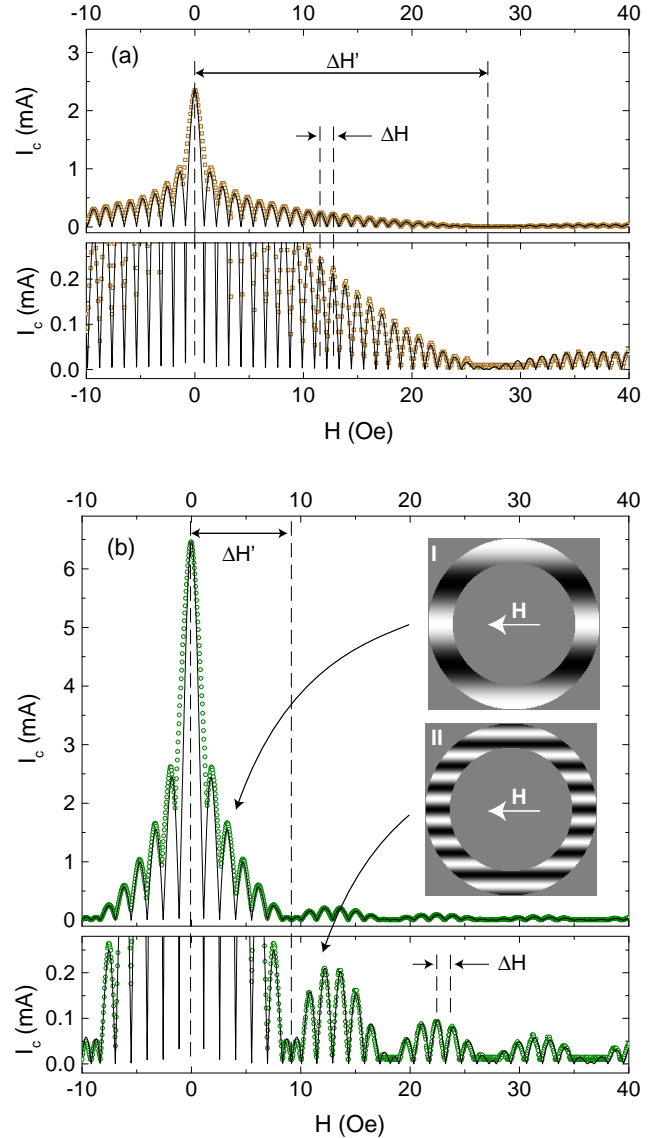


FIG. 2. Critical current diffraction patterns of (a) junction B and (b) junction D at 4.2 K. Dots are experimental data, the solid line is theory according to Eq. (2). For better visibility the low current region is also plotted on an enlarged scale. The two field modulation periods ΔH and $\Delta H'$ are indicated in each plot. The insets I and II of plot b) display the supercurrent distribution in junction D at the magnetic fields indicated by arrows; light (dark) regions correspond to current in positive (negative) direction.

where J_n is n -th Bessel function of integer order, $\delta = r_i/r_e$ is the ratio of inner radius r_i to outer radius r_e and I_0 is the maximum superconducting current at zero field. The field

$$H_0 = \Phi_0/(2\pi r_e \mu_0 \Lambda) \quad (3)$$

is the characteristic magnetic field; Φ_0 is the flux quantum, μ_0 is the vacuum permeability and Λ is the effective magnetic thickness.¹⁴

For $n = 0$, the two extreme cases $\delta \rightarrow 1$ (see Ref. 11) and $\delta \rightarrow 0$ (Ref. 8) of Eq. (2) have been discussed in the literature. The predictions of Eq. (2) have also been compared to experiments in a relatively small magnetic field range.^{4,12,15} To our knowledge, there has been no systematic comparison of the theory with experimental data for different junction width in a large field range. Our intention here is to perform such a comparison.

In Figure 2, our experimental data are fitted to Eq. (2). In the fitting procedure the values of both H_0 and δ are determined. Subsequently, the quantities acquired from the fits are labeled by a tilde ($\tilde{H}_0, \tilde{\delta}$). For the fit, the initial value of $\tilde{\delta}$ is calculated from the designed geometry of the junction; the initial \tilde{H}_0 is calculated according to Eq. (3) assuming the reasonable value of 200 nm for the magnetic thickness Λ . Then, the best fit is found by iteratively adjusting \tilde{H}_0 and $\tilde{\delta}$. The value of \tilde{H}_0 predominantly determines the small period of the critical current modulation ΔH , whereas $\tilde{\delta}$ determines the large modulation scale $\Delta H'$. This fact is in agreement with the qualitative discussion above. As can be seen from Fig. 2, excellent agreement between theory and experiment is found. The parameters $\tilde{\delta}$ and \tilde{H}_0 determined from the best fits to the data of junctions A to E are quoted in Tab. I.

Comparing the values of δ and $\tilde{\delta}$ in Tab. I, we find that $\tilde{\delta} < \delta$ for all junctions. This small but systematic deviation can be explained by assuming a symmetric deviation Δr of the junction radii from their designed dimensions (e.g., due to the photolithographic procedure during the preparation). Using this assumption, $\tilde{\delta}$ can be expressed as

$$\tilde{\delta} = \frac{r_i + \Delta r}{r_e - \Delta r}. \quad (4)$$

From the fits we find that Δr varies between 0.5 and 1.0 μm (see Tab. I). This size correction can also be explained as due to a slight over-etching of the trilayers during sample fabrication, that results in a small reduction of the sample size. The obtained Δr values agree with the size tolerance quoted by Hypres.⁷

According to theory, the quantity H_0 does only depend on the outer junction radius r_e and hence should be identical for all junctions measured. Instead, we find values of \tilde{H}_0 from the fits that slightly vary from junction to junction, see Tab. I. Using Eq. (3) the magnetic thickness $\tilde{\Lambda}$ can be calculated from \tilde{H}_0 . The values of $\tilde{\Lambda}$ obtained for each junction are quoted in the last column of Tab. I.

The average magnetic thickness is $\tilde{\Lambda} = 191 \pm 18$ nm, which is in good agreement with the value of $\Lambda \approx 2\lambda_L$ in the thick film limit, yielding a London penetration depth of $\lambda_L \approx 95$ nm.

The scatter observed in \tilde{H}_0 (or, equivalently, in $\tilde{\Lambda}$) may be due to a small number m of flux quanta threading the holes of both junction electrodes simultaneously. The critical current diffraction patterns for different values m are very similar in their qualitative features, but may differ quantitatively. Preliminary experimental results show that, upon cooling the junction from the normal to the superconducting state in a small residual magnetic field a large number of times and measuring the resulting critical current versus magnetic field, slightly different diffraction patterns depending on the value of m are observed. In such measurements we have only observed three different diffraction patterns, despite repeating the described procedure a large number of times. This strongly suggests that this effect is due to magnetic flux threading the junction loop perpendicular to the substrate.

At small fields, we observe a systematic deviation of the calculated patterns from the experimental ones. In particular, the first minimum of the critical current appears at larger field values than predicted by the theory. Moreover, the critical current at the first minimum does not fall to zero. Both facts are to be expected for junctions that are not really small in comparison with λ_J . Indeed, the dimensions of our junctions are slightly larger than λ_J . This leads to an inhomogeneous penetration of the magnetic field into the junction at low fields, resulting in an increase of the field value H at which the the first minimum of the pattern is observed. The analogous effect is observed in conventional long Josephson junctions.^{8,17}

At higher temperatures, the Josephson length λ_J increases⁸ and, hence, the effective size of the junction decreases. In the inset of Fig. 3, the calculated normalized external junction radius r_e/λ_J is plotted versus temperature, taking into account the temperature dependence of both the critical current density $j_c(T)$ and the London penetration depth $\lambda_L(T)$.⁸ At $T > 7.8$ K the normalized radius drops below unity. Therefore, at higher temperatures a better agreement between experimental data and theory can be expected at low fields. This is illustrated in Fig. 3, where the experimental critical current diffraction pattern of junction B is plotted together with a fit for the temperatures $T = 4.0, 7.0, 8.5$ K. The fit is made keeping $\tilde{\delta}$ constant for all T and adjusting \tilde{H}_0 . At elevated temperatures, both the position of the first minimum and the modulation depth of the critical current at small fields show better agreement with the theoretical prediction.

We have also measured junctions with a single fluxon trapped in the junction barrier ($n = 1$). As an example, the critical current diffraction pattern of junction B for $n = 1$ at 4.2 K is shown in Fig. 4. Taking the same fitting parameters as for the case of no trapped fluxon ($n = 0$), we find as good agreement between the theory and

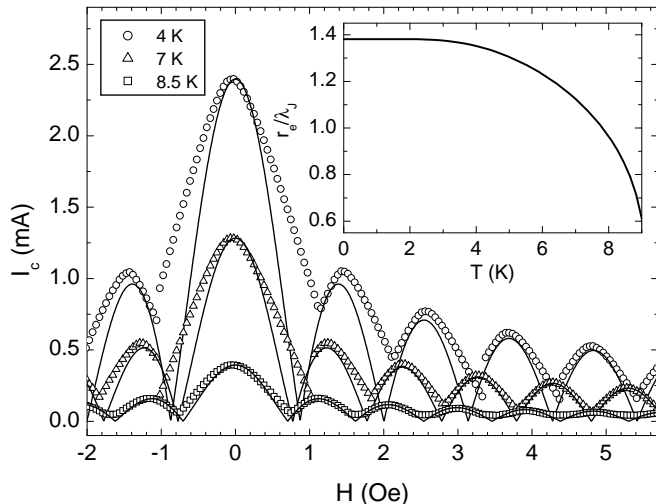


FIG. 3. Critical current diffraction patterns of junction B at temperatures between 4K and 8.5K. Dots are experimental data, solid line is theory. In the inset the calculated normalized external junction radius r_e/λ_J is plotted versus temperature.

the experimental data as before. The slight differences between the fit and the experimental data are, again, due to the dimensions ($r_e > \lambda_J$) of the junction. In the inset of Fig. 4 the supercurrent distribution in junction B at $H = 1.71$ Oe calculated according to Eq. (2) is shown. Obviously at this field a number of vortex anti-vortex pairs have penetrated into the junction but the width of the junction is not fully penetrated (compare Fig. 2b, inset II). The symmetry of the current distribution in the junction is broken due to the presence of the trapped vortex. Similar current distributions in the presence of trapped vortices have also been observed in experiment.¹⁰

It is worth to point out that good agreement between theory and experiment in the large field range is found for junctions of a diameter substantially larger than λ_J . At low fields the theory¹³ describes well the experiments with $r_e < \lambda_J$, as confirmed by our measurements at higher temperatures. Thus, the magnetic properties of the junction are determined rather by the junction radius than by the junction circumference, as already pointed out in Ref. 16.

In summary, we have systematically measured the critical current diffraction patterns of a number of annular junctions of different width, with and without trapped fluxons, in a wide magnetic field range and at different temperatures. The experimental data show a pronounced width dependence that is explained accurately using the existing theory. In particular, a modulation of the envelope of the critical current diffraction pattern is observed for junctions of large width. The period of this modulation depends very sensitively on the normalized junction size described by the parameter δ . The method of our data analysis is accurate enough to detect a small re-

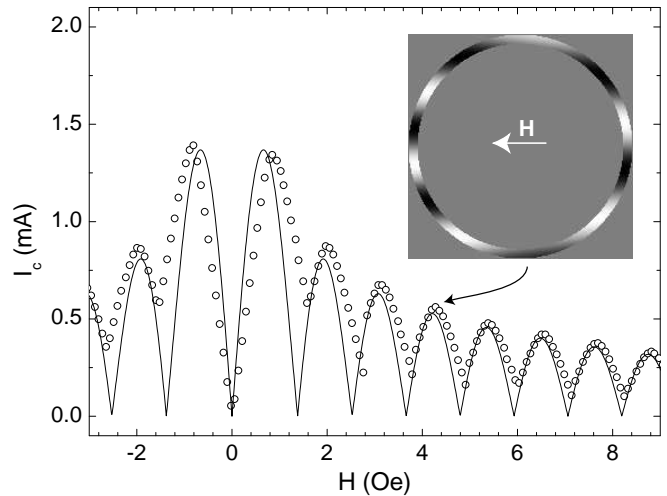


FIG. 4. Diffraction pattern of junction B with one trapped fluxon at 4.2 K. Dots are experimental data, solid line is theory. The inset displays the supercurrent distribution in the junction at the magnetic field indicated by the arrow.

duction of the size of the junction due to the fabrication process.

-
- ¹ A. V. Ustinov, *Physica D* **123**, 315 (1998).
 - ² E. Esposito, R. Cristiano, L. Parlato, and A. Barone, *Nucl. Instrum. Methods Phys. Res. A* **370**, 26 (1996).
 - ³ C. Nappi and R. Cristiano, *Appl. Phys. Lett.* **70**, 1320 (1997).
 - ⁴ R. Cristiano *et al.*, *Appl. Phys. Lett.* **74**, 3389 (1999).
 - ⁵ A. Davidson, B. Dueholm, B. Kryger, and N. F. Pedersen, *Phys. Rev. Lett.* **55**, 2059 (1985).
 - ⁶ D. W. McLaughlin and A. C. Scott, *Phys. Rev. A* **18**, 1652 (1978).
 - ⁷ Hypres Inc., Elmsford, NY 10523, U.S.A.
 - ⁸ A. Barone and G. Paterno, *Physics and Applications of the Josephson Effect* (Wiley, New York, 1982).
 - ⁹ For junction A, $\Delta H'$ was not evaluated. Due to its small width, the field necessary to observe the first minimum of the envelope of the diffraction pattern was above the range of our measurements.
 - ¹⁰ S. Keil *et al.*, *Phys. Rev. B* **54**, 14 948 (1996).
 - ¹¹ N. Martucciello and R. Monaco, *Phys. Rev. B* **53**, 3471 (1996).
 - ¹² N. Martucciello and R. Monaco, *Phys. Rev. B* **54**, 9050 (1996).
 - ¹³ C. Nappi, *Phys. Rev. B* **55**, 82 (1997).
 - ¹⁴ M. Wehlnacht, *Phys. Stat. Sol.* **32**, K169 (1969).
 - ¹⁵ C. Nappi, R. Cristiano, and M. P. Lisitskii, *Phys. Rev. B* **58**, 11 685 (1998).
 - ¹⁶ N. Martucciello *et al.*, *Phys. Rev. B* **57**, 5444 (1998).
 - ¹⁷ S. Pagano, B. Ruggiero, and E. Sarnelli, *Phys. Rev. B* **43**, 5364 (1991).